Chinese Chemical Letters xxx (2015) xxx–xxx

Contents lists available at ScienceDirect

Chinese Chemical Letters

journal homepage: www.elsevier.com/locate/cclet

Original article

A facile approach to prepare hybrid nanoparticles with morphology controlled by the thickness of glyco-shell

Wei-Yi Zhang, Guo-Song Chen *

The State Key Laboratory of Molecular Engineering of Polymers and Department of Macromolecular Science, Fudan University, Shanghai 200433, China

ARTICLE INFO

Article history:
Received 1 April 2015
Received in revised form 28 April 2015
Accepted 5 May 2015
Available online xxx

Keywords:
Glycopolymer
Self-assembly
Gold nanoparticles
Morphology

ABSTRACT

Herein, we designed a novel amphiphilic triblock glycopolymer poly(oligo(ethyleneglycol) methacrylate)-block-poly(maltopyranoside methacrylate)-block-polystyrene (POMA-*b*-PMal-*b*-PS) *via* the combination of reversible addition-fragmentation chain transfer (RAFT) polymerization and post-polymerization modification. The micelles with core–shell–corona structures were prepared by direct self-assembly of this glycopolymer in water. We found that these micelles can be used in *in situ* formation and stabilization of AuNPs. By controlling the thickness of glyco-shell, we successfully obtained Janus particles and raspberry-like particles with AuNPs in the sugar shell.

1. Introduction

Glycopolymers are synthetic polymers featuring pendant carbohydrate moieties on a non-carbohydrate main chain [1]. Their good water solubility, low toxicity and biocompatibility render them a wide range of applications, such as drug delivery [2], vaccines [3], fluorescent probes [4], *etc*. To further extend these bio-applications to a much boarder area, one feasible method is to hybridize them with inorganic nanomaterials [5,6]. The corresponding "sweet" hybrid nanomaterials have shown great promise in the areas of sensor [7], magnetic resonance imaging [8] and vaccines [3], which made them receive quite a few attentions.

However, in most cases, thiol-functionalized glycopolymers were directly bound to gold nanoparticles (AuNPs) *via* Au–S bond. When surface of AuNP is covered with thiol-containing polymers, the nanoparticle only provides a scaffold and the property of AuNP itself could not be fully incorporated [9]. One convenient way to solve this problem is to stabilize AuNPs without using thiol group. In literature, monosaccharide on the surface of dendrimers was proved to stabilize AuNPs in water [10]. Recently, we also have demonstrated that AuNPs can be generated *in situ* and stabilized by glyco-inside vesicles [11]. This study provided a new route to generate rather "free" AuNPs within self-assembled micelles or vesicles, which might be beneficial for their further bio-applications. But in these studies, full manipulation on morphology of the hybrid nanomaterial was not achieved, which might hamper our further exploration. Thus, this paper aims at generating nanomaterials stabilized by glycopolymers with precise control on the morphology. By controlling the thickness of glyco-shell, Janus "sweet" nanoparticle was realized, which has not been reported in literature. In the end, catalysis property of these nanomaterials was also investigated.

2. Results and discussion

2.1. Synthesis and characterization of triblock glycopolymers

To control the morphology of hybrid nanomaterials [12] and even make Janus ones, polymer scientists have developed some intelligent strategies [13–15]. Among them, properties of the polymeric micelles, including the lengths of different stabilizing blocks and softness of stabilizing micelle cores were also employed [16]. However, glyco-NPs have not been utilized for preparation of Janus hybrid particles. Considering the bulky sugar pendant groups on the main chain of glycopolymers, we suppose that the effect from glyco-block might be much more significant than the previous non-sugar units. Thus two tri-block copolymers are designed, *i.e.* their middle blocks are glyco-blocks with hydrophobic and hydrophilic blocks on their both sides. By controlling the ratio between the sugar block and the hydrophobic block, different

* Corresponding author.
E-mail address: guosong@fudan.edu.cn (G.-S. Chen).

http://dx.doi.org/10.1016/j.cclet.2015.05.022
1001-8417/

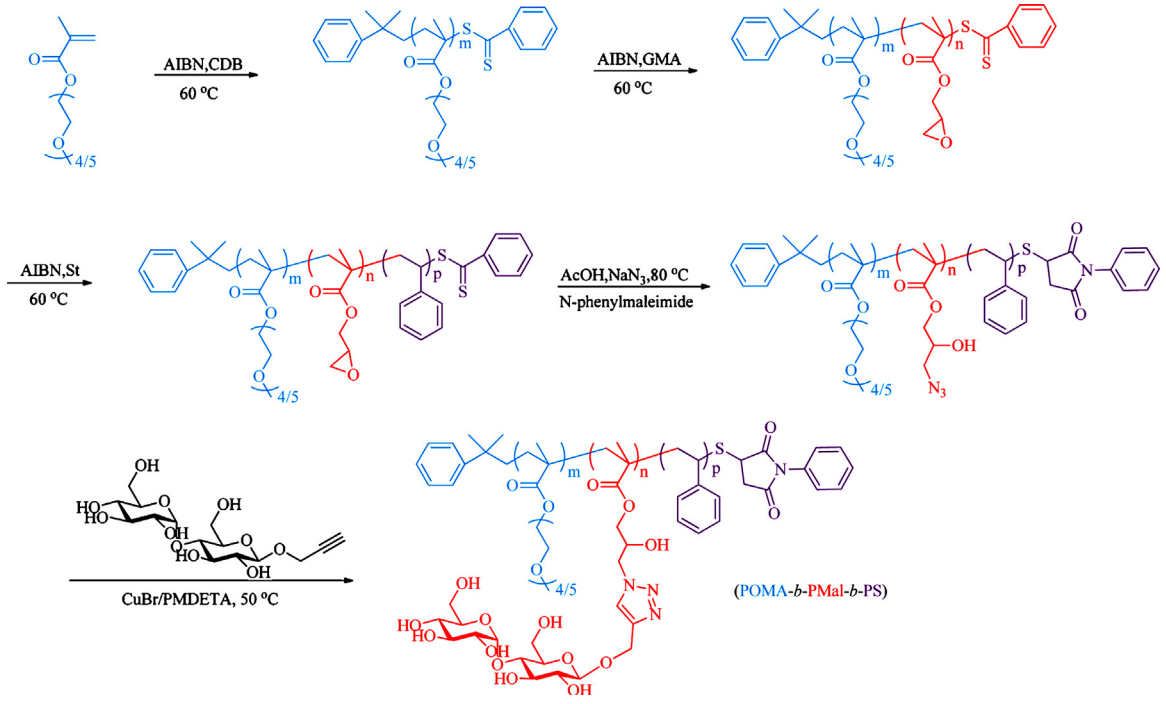

Scheme 1. Synthetic route of amphiphilic triblock glycopolymer POMA-*b*-PMal-*b*-PS.

morphologies of hybrid nanomaterials (glyco-AuNPs) were expected after *in situ* reduction of precursor $HAuCl_4$.

Glycopolymers were synthesized *via* the combination of reversible addition–fragmentation chain transfer (RAFT) polymerization and post-polymerization modification. As shown in Scheme 1, the triblock glycopolymer contains three components, from left to right, a hydrophilic poly(oligo(ethyleneglycol) methacrylate) (POMA) block, a hydrophilic glyco-block (PMal) and a hydrophobic polystyrene block (PS). The length of POMA in the two series of triblock glycopolymers was similar. However, the ratio of PMal:PS was designed to vary, which might help us to demonstrate the contribution of the middle glyco-block.

Briefly, oligo(ethylene glycol) methacrylate (OMA, M_n = 300 g mol^{-1}) was polymerized by RAFT polymerization using cumyl dithiobenzoate (CDB) as chain transfer agent (CTA), yielding **P1**-1 and **P2**-1. As shown in Table 1, the degree of polymerization (DP) of POMA was obtained by comparison of the integral areas of ethylene glycol peak at 4.02 ppm and that of the phenyl group of CTA at 7.0–8.0 ppm in ^{1}H NMR. Then, the obtained POMA was used as macro chain transfer agent (macro-CTA) to prepare the second block poly(glycidyl methacrylate) (PG), yielding two diblock copolymers **P1**-2 and **P2**-2. Similarly, the DP of PG block was calculated by comparing the ^{1}H NMR peak of epoxy unit of PG at 2.64 ppm and that of ethylene glycol at 4.02 ppm. The triblock copolymer POMA-*b*-PG-*b*-PS was further prepared using the previous diblock copolymer (**P1**-2 and **P2**-2) as macro-CTA and styrene as monomer, yielding **P1**-3 and **P2**-3, with their DP obtained from the integral area of PS at 6.5–7.5 ppm. All of these copolymers showed narrow polydispersity indexes (PDI), measured by gel permeation chromatography (GPC). And the characterization results are shown in Table 1 and Figs. S1 and S2 in Supporting information. It is worth to mention that ^{1}H NMR results were used to determine DP, since PEG was used as calibration standard for GPC analysis, which was not effective to characterize glycopolymers due to great structural inconsistency.

Table 1
M_n and PDI of precursors of the final triblock copolymers.

Polymers	M_n (^{1}H NMR)	M_w/M_n (GPC)
$POMA_{22}$ (**P1**-1)	6600	1.21
$POMA_{22}$-*b*-PG_{54} (**P1**-2)	14,270	1.21
$POMA_{22}$-*b*-PG_{54}-*b*-PS_{17} (**P1**-3)	16,000	1.31
$POMA_{20}$ (**P2**-1)	6000	1.12
$POMA_{20}$-*b*-PG_{26} (**P2**-2)	9700	1.13
$POMA_{20}$-*b*-PG_{26}-*b*-PS_{108} (**P2**-3)	21,000	1.36

Combination of ring-opening reaction and click reaction was used in post-polymerization modification. **P1**-3 and **P2**-3 were treated with NaN_3 and acetic acid at 80 °C to obtain azide-containing copolymer **P1**-4 or **P2**-4, by the ring opening of epoxide from the glycidyl methacrylate. Disappearance of the epoxy units in ^{1}H NMR spectra and the appearance of azide at 2105 cm^{-1} in Fourier transform infrared spectra (FT-IR) demonstrated the complete transformation from epoxide to azide (Fig. S3 in Supporting information). After click reaction with propargyloxy-*β*-maltopyranoside, the strong peak of azide at 2105 cm^{-1} disappeared (Fig. S3), while the peak at 3340 cm^{-1} increased due to the hydroxyl groups from maltose. This result indicated the complete conversion to POMA-*b*-PMal-*b*-PS. ^{1}H NMR was also used to characterize the triblock glycopolymers (Fig. S3). Finally, a pair of triblock glycopolymers was determined as $POMA_{22}$-*b*-$PMal_{54}$-*b*-PS_{17} (**P1**) with PMal to PS ratio as 3:1, and $POMA_{20}$-*b*-$PMal_{26}$-*b*-PS_{108} (**P2**) with PMal to PS ratio as 1:4. As control, $POMA_{22}$-*b*-PPA_{54}-*b*-PS_{17} (**P3**) was obtained by the same strategy but propargyl alcohol was used to click with azide-containing polymer **P1**-4 (FT-IR and ^{1}H NMR in Fig. S4 in Supporting information) instead. What is more, diblock copolymer $PMal_{47}$-*b*-PS_{158} (**P4**) was also synthesized (GPC, FT-IR and ^{1}H NMR characterization data are shown in Fig. S5 and S6) *via* the similar strategy and used as another control.

2.2. Preparation of glyco-NPs

Self-assembly of glycopolymers were performed by selective solvent method. Typically **P1** or **P2** was firstly dissolved in 1 mL DMAc (dimethylacetamide, 10 mg mL^{-1}), then 8 mL deionized water was added into the solution quickly. After dialysis, the final concentration was fixed at 0.83 mg mL^{-1} in which self-assembled

Please cite this article in press as: W.-Y. Zhang, G.-S. Chen, A facile approach to prepare hybrid nanoparticles with morphology controlled by the thickness of glyco-shell, Chin. Chem. Lett. (2015), http://dx.doi.org/10.1016/j.cclet.2015.05.022

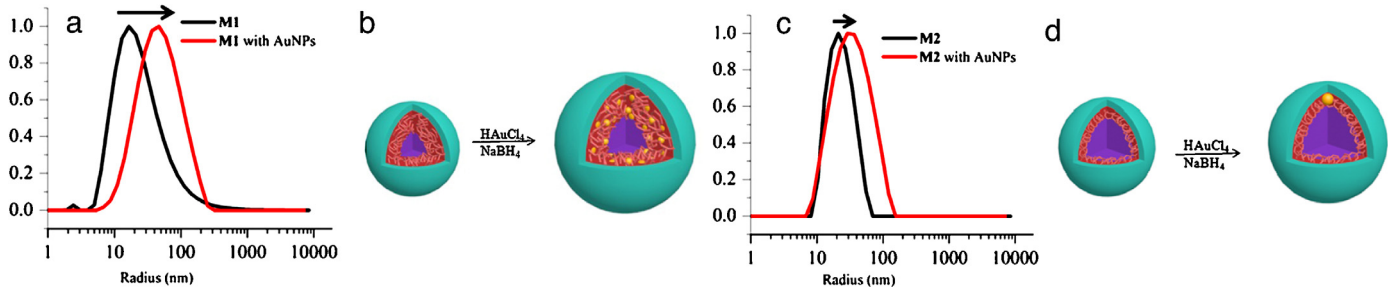

Fig. 1. (a) DLS and (b) cartoon scheme of **M1** before and after reduction of $HAuCl_4$; (c) DLS and (b) cartoon scheme of **M2** before and after reduction of $HAuCl_4$.

structures were obtained. For clarity, **M1** and **M2** were used to represent the nanostructures formed by the corresponding glycopolymer precursors **P1** and **P2**, respectively. Dynamic light scattering (DLS) and transmission electron microscopy (TEM) were used to characterize these structures (Fig. 1 and Fig. S7 in Supporting information). DLS measurements showed that $\langle R_h \rangle$ (hydrodynamic radius) of **M1** and **M2** was 18 nm and 20 nm, respectively. TEM pictures confirmed their micellar morphologies (Fig. S7). According to the chemical structure of **P1** and **P2**, **M1** and **M2** were proposed as micelles with PS as the dense core, soluble glyco-block PMal as the shell, and short POMA as the corona outside the shell. **M1** and **M2** at the same concentration were characterized by ^{1}H NMR with equal amount of sodium 2,2-dimethyl-isotope 2-silapentane-5-sulfonate (DSS) as internal standard. As shown in Fig. S8 in Supporting information, the integral ratio of triazole group (**M1** to **M2**), as a marker of sugar moieties was about 2.5:1. This result indicated that the amount of solvated sugar units from **M1** were much larger than that of **M2** in water, demonstrating the glyco-shell of **M1** was thicker than that of **M2** as we designed, although their overall $\langle R_h \rangle$ seemed similar. Similarly, **M3** and **M4** formed micelles with $\langle R_h \rangle$ around 30 nm and 26 nm, respectively (Fig. S9 in Supporting information).

2.3. *In situ* formation of Glyco-AuNPs

M1 and **M2** were used for *in situ* AuNP formation. Chloroauric acid ($HAuCl_4$) was firstly mixed with the glyco-NPs by stirring at room temperature overnight. UV–vis spectrum of the mixture proved that no self-reduction happened during this process (Fig. S10 in Supporting information). Then $NaBH_4$ (3.2 equiv. to $HAuCl_4$) was then added and the mixture turned brown in several seconds. Appearance of a distinct characteristic absorption peak at 515 nm in the UV–vis spectrum (Fig. S11 in Supporting information) confirmed the formation of AuNPs. TEM images also demonstrated the presence of AuNPs, i.e. the black dots with diameters smaller than 10 nm (Fig. 2). The magnified images of the AuNPs showed an obvious crystal lattice and the inter-planar spacing of the lattice was near 0.224 nm (Fig. 2b and d), which agreed well with the (1 1 1) lattice spacing of AuNPs. The EDX (energy dispersive X-ray) spectrum showed that there were strong peaks for elemental gold indicating that these nanoparticles were composed of Au (Fig. S12 in Supporting information). It was quite interesting to find that **M1** with a thick sugar shell had many AuNPs with diameter around 3 nm (Fig. 2a and b with inset cartoon). While most of **M2** with thin sugar shells had only one AuNP with diameter around 7 nm (Fig. 2c and d with inset cartoon), demonstrating the feature of Janus particles. This "one-micelle-one-AuNP" hybrid structure could be easily found under TEM (Fig. 2c and d) and more TEM images were presented in Fig. S13 in Supporting information. Interestingly, after reduction of $HAuCl_4$, the $\langle R_h \rangle$ of **M1** increased to 43 nm (Fig. 1) compared to the original 18 nm. However, the $\langle R_h \rangle$ of hybridized **M2** kept constant, which was around 27 nm. As a control, by using triblock copolymer **P3** with the same backbone but no sugar inside, the micelle **M3** could not stabilize AuNPs, which were much larger than those inside the glyco-micelles and easily aggregated (Fig. S14 in Supporting information). Moreover, the same experiment was carried out for micelles formed by diblock copolymer without POMA (**P4**), resulting in precipitates after reduction (Fig. S15 in Supporting information). Therefore, this result indicated that the three-layer design of micelles with the glyco-layer in the middle was crucial to stabilize AuNPs.

To investigate the role of glyco-shell thickness in nanoparticle hybridization, different amounts of $HAuCl_4$ were employed to form glyco-AuNPs, while the amount of the glyco-NPs and reducing reagent $NaBH_4$ were constant. To the aqueous solution of glyco-NPs (1 mL, 0.83 mg mL^{-1}), different amount of $HAuCl_4$ (50 mg mL^{-1}) was added (1 μL, 5 μL and 10 μL), followed by incubation and reduction. As shown in Fig. S16 in Supporting information, the size of AuNPs encapsulated by **M1** was all around 3 nm (Fig. S16(a)–(c)), and more AuNPs were found inside the micelles with the increasing concentration of $HAuCl_4$. On the contrary, the encapsulated amount of AuNPs by **M2** only slightly increased with increasing concentration of $HAuCl_4$ (Fig. S16(d)–(f)). The result indicated that the Janus particle morphology was greatly related to the thickness of glyco-shell, not directly determined by the concentration of $HAuCl_4$ and $NaBH_4$. At an appropriate concentration of $HAuCl_4$ and $NaBH_4$, Janus particles would be observed in the presence of **M2** (Fig. 2c and d). For the

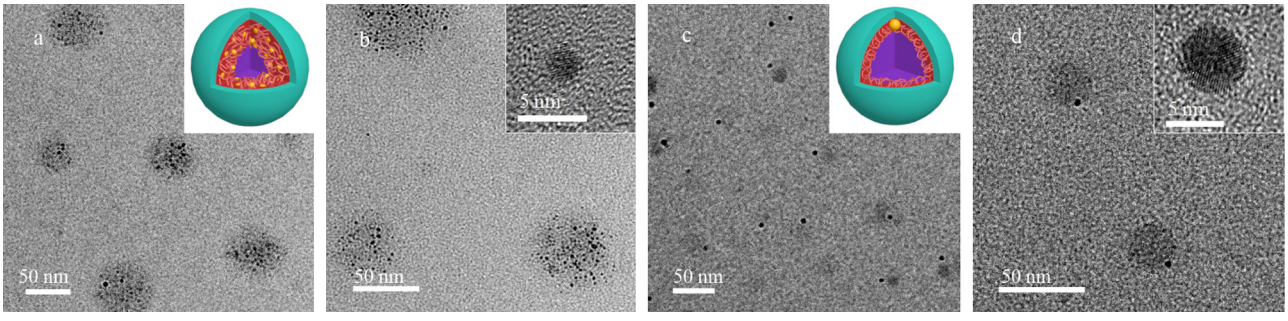

Fig. 2. TEM images of different glyco-AuNPs. (a), (b) **M1** with many AuNPs inside (inset: cartoon scheme); (c), (d) **M2** with only one AuNP inside (inset: cartoon scheme).

Please cite this article in press as: W.-Y. Zhang, G.-S. Chen, A facile approach to prepare hybrid nanoparticles with morphology controlled by the thickness of glyco-shell, Chin. Chem. Lett. (2015), http://dx.doi.org/10.1016/j.cclet.2015.05.022

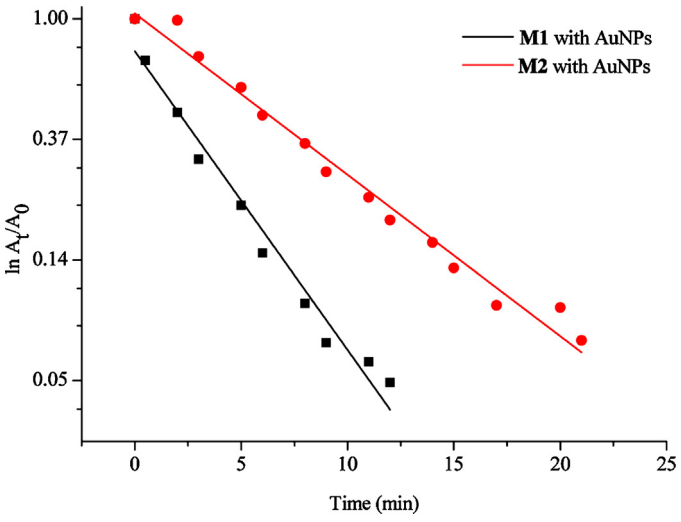

Fig. 3. Plot of $\ln(A_t/A_0)$ *versus* time for the reduction of 4-NP. Black line: **M1** with AuNPs; Red line: **M2** with AuNPs.

mechanism, we supposed that $HAuCl_4$ might locate in the sugar layer and protected by the POMA corona. After reduction, if the sugar layer was very thin, only a few Au seeds could be loaded in the shell and only one seed can grow up forming nanoparticle. However, when the sugar shell became thicker, more Au seeds would be inside the shell resulting in formation of much more AuNPs.

2.4. Catalytic reduction of 4-nitrophenol (4-NP)

To evaluate the catalytic activity of the glyco-AuNPs, model reduction reaction of 4-nitrophenol (4-NP) to 4-aminophenol (4-AP) in the presence of an excess amount of $NaBH_4$ was studied. AuNPs were widely used as catalyst for this reaction (Fig. S17 in Supporting information) by relaying electrons from donor BH_4^- to acceptor 4-NP [17], when both of them were adsorbed on surface. The reaction process was monitored by UV–vis spectrometry. As shown in Fig. S18c in Supporting information, the reaction could not happen in the absence of glyco-AuNPs. After addition of the catalyst, the characteristic peak of 4-NP at 400 nm started to decrease, while a new peak of 4-AP at 295 nm appeared (Fig. S18). After a while, the peak of 4-NP was no longer observed and the solution color changed from yellow to colorless, indicating that the catalytic reduction of 4-NP proceeded completely. The rate constant k was calculated using the rate law for the first-order kinetics: $\ln(A_t/A_0) = -kt$, where A_t represented absorbance of 4-NP at any time, A_0 represented the starting absorbance of 4-NP and k was rate constant. Fig. 3 showed a good linear correlation of $\ln(A_t/A_0)$ *versus* time, therefore the kinetic reaction rate constant was estimated as $4.0 \times 10^{-3}\ s^{-1}$ for **M1** and $2.2 \times 10^{-3}\ s^{-1}$ for **M2**. Both the them were larger than citrate-capped AuNPs ($1.2 \pm 0.1 \times 10^{-3}\ s^{-1}$) with diameter of 3.5 nm and poly(*N*-isopropylacrylamide)-*b*-poly(4-vinyl pyridine) (PNIPAM-*b*-P4VP) stabilized AuNPs ($1.5 \times 10^{-3}\ s^{-1}$) with diameter of 3.3 nm, which located in the dense core of P4VP [18,19].

3. Conclusion

A novel amphiphilic brush triblock glycopolymer POMA-*b*-PMal-*b*-PS was prepared through the combination of RAFT polymerization and post-polymerization modification. Micelles prepared by this new glycopolymer were used to *in situ* formation of AuNPs. Different morphologies including Janus particles and raspberry-like particles were obtained by changing the ratio of PMal and PS.

Acknowledgments

Ministry of Science and Technology of China (No. 2011CB932503332), National Natural Science Foundation of China (No. 91227203, 21474020 and 51322306), and the Shanghai Rising-Star Program (No. 13QA1400600) are acknowledged for their financial support.

Appendix A. Supplementary data

Supplementary data associated with this article can be found, in the online version, at http://dx.doi.org/10.1016/j.cclet.2015.05.022.

References

[1] A. Ghadban, L. Albertin, Synthesis of glycopolymer architectures by reversible-deactivation radical polymerization, Polymers 5 (2013) 431–526.
[2] C. Zheng, Q.Q. Guo, Z.M. Wu, et al., Amphiphilic glycopolymer nanoparticles as vehicles for nasal delivery of peptides and proteins, Eur. J. Pharm. Sci. 49 (2013) 474–482.
[3] A.L. Parry, N.A. Clemson, J. Ellis, et al., 'Multicopy Multivalent' glycopolymer-stabilized gold nanoparticles as potential synthetic cancer vaccines, J. Am. Chem. Soc. 135 (2013) 9362–9365.
[4] T. Xing, X.Z. Yang, L.Y. Fu, L.F. Yan, Near infrared fluorescence probe and galactose conjugated amphiphilic copolymer for bioimaging of HepG2 cells and endocytosis, Polym. Chem. 4 (2013) 4442–4449.
[5] M.H. Mashhadizadeh, R.P. Talemi, Application of diazo-thiourea and gold nanoparticles in the design of a highly sensitive and selective DNA biosensor, Chin. Chem. Lett. 26 (2015) 160–166.
[6] X.H. Lv, L.P. Wang, G. Li, et al., Preparation and characterization of optically functional hollow sphere hybrid materials by surface-initiated RATRP and "click" chemistry, Chin. Chem. Lett. 24 (2013) 335–337.
[7] M. Takara, M. Toyoshima, H. Seto, Y. Hoshino, Y. Miura, Polymer-modified gold nanoparticles *via* RAFT polymerization: a detailed study for a biosensing application, Polym. Chem. 5 (2014) 931–939.
[8] A. Pfaff, A. Schallon, T.M. Ruhland, et al., Magnetic and fluorescent glycopolymer hybrid nanoparticles for intranuclear optical imaging, Biomacromolecules 12 (2011) 3805–3811.
[9] K. Kuroda, T. Ishida, M. Haruta, Reduction of 4-nitrophenol to 4-aminophenol over Au nanoparticles deposited on PMMA, J. Mol. Catal. A: Chem. 298 (2009) 7–11.
[10] K. Esumi, T. Hosoya, A. Suzuki, K. Torigoe, Spontaneous formation of gold nanoparticles in aqueous solution of sugar-persubstituted poly(amidoamine) dendrimers, Langmuir 16 (2000) 2978–2980.
[11] L. Su, C.M. Wang, F. Polzer, et al., Glyco-inside micelles and vesicles directed by protection–deprotection chemistry, ACS Macro Lett. 3 (2014) 534–539.
[12] Y.X. Zhang, X.D. Hao, Z.P. Diao, Templated self-assembly of Au–TiO_2 binary nanoparticles–nanotubes, Chin. Chem. Lett. 25 (2014) 874–878.
[13] T. Chen, M.X. Yang, X.J. Wang, L.H. Tan, H.Y. Chen, Controlled assembly of eccentrically encapsulated gold nanoparticles, J. Am. Chem. Soc. 130 (2008) 11858–11859.
[14] J. He, M.T. Perez, P. Zhang, et al., A general approach to synthesize asymmetric hybrid nanoparticles by interfacial reactions, J. Am. Chem. Soc. 134 (2012) 3639–3642.
[15] W.P. Li, V. Shanmugam, C.C. Huang, et al., Eccentric inorganic-polymeric nanoparticles formation by thermal induced cross-linked esterification and conversion of eccentricity to raspberry-like Janus, Chem. Commun. 49 (2013) 1609–1611.
[16] N. Ali, S.Y. Park, Micellar structures of poly(styrene-*b*-4-vinylpyridine)s in THF/Toluene mixtures and their functionalization with gold, Langmuir 24 (2008) 9279–9285.
[17] T. Premkumar, K. Lee, K.E. Geckeler, Shape-tailoring of gold nanostructures: can a detergent act as the reducing or protecting agent? Nanoscale 3 (2011) 1482–1484.
[18] R. Fenger, E. Fertitta, H. Kirmse, A.F. Thünemann, K. Rademann, Size dependent catalysis with CTAB-stabilized gold nanoparticles, Phys. Chem. Chem. Phys. 14 (2012) 9343–9349.
[19] Y. Wang, G.W. Wei, W.Q. Zhang, et al., Responsive catalysis of thermoresponsive micelle-supported gold nanoparticles, J. Mol. Catal. A: Chem. 266 (2007) 233–238.

Please cite this article in press as: W.-Y. Zhang, G.-S. Chen, A facile approach to prepare hybrid nanoparticles with morphology controlled by the thickness of glyco-shell, Chin. Chem. Lett. (2015), http://dx.doi.org/10.1016/j.cclet.2015.05.022